Macromolecules 1993, 26, 6338–6345

Synthesis, Characterization, and Surface Structures of Styrene–2-Vinylpyridine–Butadiene Three-Block Polymers

Hiroshi Watanabe,[*,†] **Takatoshi Shimura,**[†] **Tadao Kotaka,**[†] **and Matthew Tirrell**[‡]

Department of Macromolecular Science, Faculty of Science, Osaka University, Toyonaka, Osaka 560, Japan, and Department of Chemical Engineering and Materials Science, University of Minnesota, Minneapolis, Minnesota 55455

Received February 23, 1993; Revised Manuscript Received August 18, 1993[®]

ABSTRACT: For the purpose of studying morphologies of ultra-thin adsorbed layers, novel polystyrene–poly(2-vinylpyridine)–polybutadiene (PS–PVP–PB) three-block polymers were synthesized with a multistep coupling method. First, end-chlorinated PS–PVP-Cl diblock precursors were made via termination of living PS–PVP$^-$ anions with a large excess of *p*-xylylene dichloride (XDC). Those PS–PVP-Cl precursors were precipitated in heptane under vacuum to reduce substantially the amount of unreacted XDC left with them and then were allowed to be coupled with PB precursors having diphenylethylene (DPE) anion ends. The desired 1:1 coupling of the PS–PVP-Cl and PB–DPE$^-$ precursors was successfully achieved, and the PS–PVP–PB three-block polymers were obtained after fractionation. Preliminary surface measurements were carried out for ultra-thin, adsorbed layers of some of those PS–PVP–PB polymers. Those layers were prepared on mica, and were examined in their as-dried state without any heat treatment. X-ray photoelectron spectroscopy and contact angle measurements revealed that the PVP blocks were located at the bottom of the layers while the PS and PB blocks were at the top. Surface profiles of the top layers were examined with an atomic force microscope (AFM), and nodules of height ≅ 1 nm and width ≅ 20–50 nm were observed. Similar nodules were found for an adsorbed layer of a PS–PVP diblock polymer, but not for a PB–PVP layer. This result suggested that the nodules for the PS–PVP–PB layers were the domains of the PS blocks. Mechanisms of the nodule formation as well as the location of the PB blocks in the PS–PVP–PB adsorbed layers are discussed.

I. Introduction

One of the most prominent features of block polymers is formation of microdomains.[1] Extensive studies have been made on bulk block polymers in the strongly segregated state, and the thermodynamic origin of morphologies is well understood.[2–5] The block polymer chains have to satisfy some contradicting requirements, e.g., an osmotic requirement of uniform segment distribution in each domain and an elastic requirement of randomized block conformations. In this sense, the block polymers are thermodynamically confined, so that they have non-Gaussian conformations[6] and exhibit unique morphologies (spheres, cylinders, bicontinuous diamonds, or lamellae) that are determined by a balance of all those requirements.[4,5] Effects of this thermodynamic confinement are expected to be stronger for block polymers in *ultra-thin* layers (with the thickness ≪ unperturbed dimensions of the constituent blocks) than in bulk systems, because the block polymers have very little conformational freedom in the thin layer and also because they interact with substances in contact with the layer. The resulting morphologies of the thin layers might be quite different from those in bulk and are the subject of our interest.

Nevertheless, the block polymer morphologies in ultra-thin layers have been hardly investigated, partly because of a lack of good model systems. As a polymer that can form the model layers, we here consider polystyrene (PS)–poly(2-vinylpyridine) (PVP)–polybutadiene (PB) three-block polymers for the following reason. It is well known that PS–PVP and polyisoprene (PI)–PVP diblock polymers are adsorbed on mica to form ultra-thin layers (of typical thickness ≅ a few nanometers) in dry states.[7,8] In those layers, the adsorbed PVP blocks are located at the bottom, and the nonadsorbed PS or PI blocks are at the top.[7,8] Since PB blocks are very similar to the PI blocks, we expect that the PS–PVP–PB three-block polymers also form ultra-thin adsorbed layers on mica: The PVP blocks should be at the bottom and vertically segregate from the PS and PB blocks. The PS and PB blocks would further segregate either vertically or laterally in the top part of the dried, absorbed layer, in distinction to the structure of the PS–PVP or PI–PVP layers having only one component (PS or PI) at the top. In some sense, the top part of the PS–PVP–PB polymer layers is regarded as a layer of a PS–PB diblock polymer with its junction being anchored on the substrate, and interesting structures are expected to be formed.

From the above point of view, we have attempted to synthesize novel PS–PVP–PB three-block polymers and examine the structures of their adsorbed layers on mica. Differing from PS–PB–*PVP* block polymers having the PVP block at the end,[9] we cannot make the PS–*PVP*–PB polymers with a routine method of sequential anionic polymerization because the living PVP anions do not initiate the polymerization of PS and PB blocks.[10,11] Thus, we have synthesized the PS–PVP–PB polymers with a newly developed multistep coupling method and have carried out preliminary surface measurements on their adsorbed layers. This paper explains the method of synthesis and results of the measurements.

II. Experimental Section

II-1. Synthesis. PS–PVP–PB three-block polymer samples were prepared with the multistep coupling method explained below and PB–PVP and PS–PVP diblock polymers by sequential anionic polymerization. All reactions were carried out under high vacuum with glass flasks and breakable seals. Standard methods of purification[10,11] were applied to all *monomers*, styrene (S), butadiene (B), 2-vinylpyridine (VP), and diphenylethylene

---

[†] Osaka University.

[‡] University of Minnesota.

[®] Abstract published in *Advance ACS Abstracts*, October 15, 1993.

0024-9297/93/2226-6338$04.00/0

Scheme I. Synthesis of PS–PVP–PB Three-Block Polymers with a Multistep Coupling Method[a]

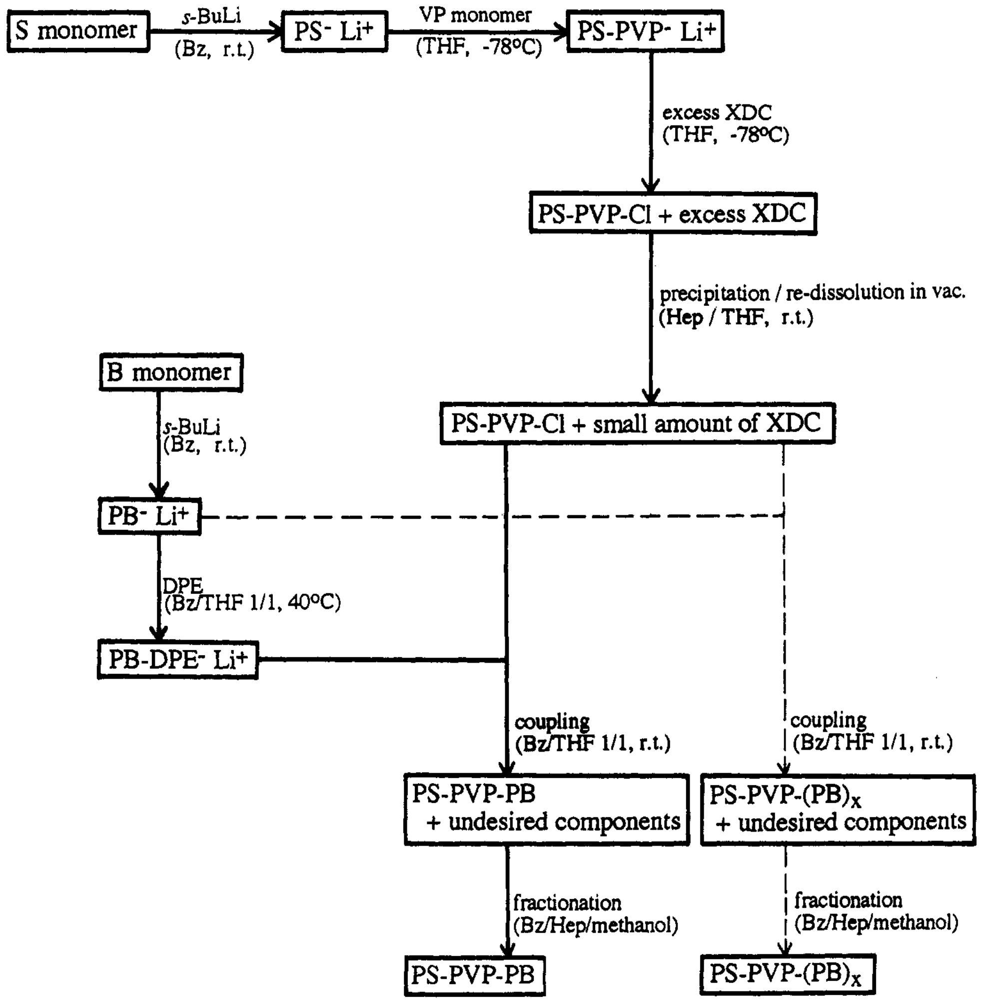

[a] The solid arrows indicate the successful path used in this study.

(DPE; used for end-modification of PB precursors explained later), *solvents*, benzene (Bz), tetrahydrofuran (THF), and heptane (Hep), and *terminators*, methanol and *p*-xylylene dichloride. The initiator, *sec*-butyllithium (*s*-BuLi), was made from lithium metal and *sec*-butyl chloride according to the method suggested by Fujimoto.[10]

Preparation of PS–PVP-Cl Precursor. As shown in Scheme I, living PS anions were first synthesized in Bz (to ensure narrow molecular weight distribution), the solvent was switched to THF via vacuum distillation, and then the PVP blocks were copolymerized to obtain a PS–PVP⁻/THF solution (with C_{PS-PVP} = 1–2 wt %). To this solution, vigorously stirred at −78 °C, a large excess of *p*-xylylene dichloride (XDC) diluted with THF was added through a shower inlet. Immediately after the addition, the termination was completed and the PS–PVP-Cl diblock precursors having benzyl chloride groups $PhCH_2Cl$ at the PVP ends were obtained.

The resulting PS–PVP-Cl/THF solution (recovered in a flask under vacuum) contained a large amount of unreacted (excess) XDC. For removal of XDC, the PS–PVP-Cl precursors had to be precipitated in Hep (a nonsolvent for both PS and PVP blocks) and then redissolved in THF. If this precipitation/redissolution procedure is carried out under atmospheric conditions, water and other impurities contaminate the precursors. Thus, we used an apparatus shown in Figure 1 and carried out the procedure under *high vacuum*: The PS–PVP-Cl/THF solution ($\simeq$100 mL in the flask F1) was first introduced into the flask M, and the whole apparatus was tilted to transfer $\simeq$350 mL of pure Hep from the flask H to M. The resulting mixture was vigorously stirred for $\simeq$20 min and kept at rest until the PS–PVP-Cl precursors completely precipitated. Then, the apparatus was slowly tilted to transfer the supernatant (containing the excess XDC) from M to H. Finally, pure THF was drained from the flask T to M to redissolve the precursors, and the flask H was sealed off.

The PS–PVP-Cl/THF solution left in the flask M still contained a small amount of XDC, but it did not significantly disturb the subsequent coupling reaction with living PB precursors. The solution was transferred and sealed in the flask F2, divided from F2 into some ampoules, and stored in a deep freezer until use.

Coupling of PS–PVP-Cl and PB–DPE Precursors. Coupling of PB anions and the PS–PVP-Cl precursors was disturbed by a side reaction explained later in Figure 2. Thus, as shown in Scheme I, the PB anion ends were converted to DPE anions through a reaction with a prescribed amount of DPE monomers (2-4 times excess to the PB⁻ ends). Then, the resulting PB–DPE⁻ precursors were allowed to couple with the PS–PVP-Cl precursors in a 1/1 Bz/THF mixed solvent at $\simeq$25 °C for 24-48 h. A large excess of the PB–DPE⁻ precursors was used to enhance the coupling of chemically different chains. As demonstrated later in Figure 2, the side reaction was efficiently supressed for the end-modified PB–DPE⁻ precursors.

Fractionation. In addition to the desired PS–PVP–PB polymers, the crude product of the coupling reaction contained unreacted (excess) PB–DPE precursors, $(PB–DPE)_2$ dimers formed by bimolecular termination of PB–DPE⁻ precursors by XDC (left in the PS–PVP-Cl solution), a trace amount of graft-block polymers explained later, and unreacted PS–PVP-Cl precursors when coupling with a high molecular weight PB–DPE precursor was attempted. To remove these undesired components, we fractionated the crude product at 25–45 °C from Bz/Hep/methanol ternary solvents of composition $\simeq$2/8/1. (We also mixed cyclohexane in the solvents when we had the unreacted PS–PVP-Cl precursors.) Because of large differences of the solubilities of PS, PB, and PVP blocks, the undesired components were rather easily removed after several fractionation steps.

II-2. Characterization. All precursors (recovered whenever necessary) and the reaction products were characterized by gel permeation chromatography (GPC; Tosoh HLC-8) employing a

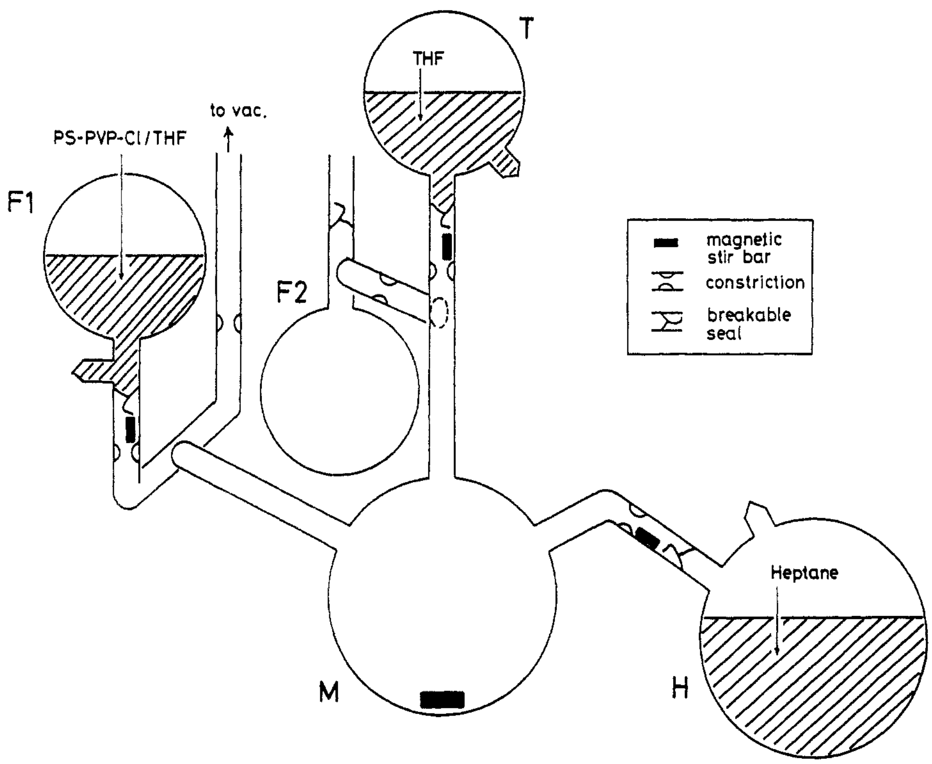

Figure 1. Schematic illustration for an apparatus used for the precipitation/redissolution procedure under vacuum. Glass flasks (500 mL) were used for M and H and 200- or 300-mL flasks for F1, F2, and T.

Table I. Characteristics of PS–PVP–PB Three-Block Polymers

	precursor PS[a]		precursor PS–PVP[b]		precursor PB[a]		PS–PVP–PB[c]	
code	$10^{-3}M_{PS}$	$(M_w/M_n)_{PS}$	$10^{-3}M_{PVP}$	$(M_w/M_n)_{PS\text{-}PVP}$	$10^{-3}M_{PB}$	$(M_w/M_n)_{PB}$	$10^{-3}M_{PB}^{calc}$	$(M_w/M_n)_{PS\text{-}PVP\text{-}PB}$
PS–PVP–PB 39-57-15	38.5	1.05	57.0	1.08	14.6	1.05	15.7	1.09
PS–PVP–PB 39-57-39	38.5	1.05	57.0	1.08	38.5	1.07	41.1	1.07
PS–PVP–PB 39-57-89	38.5	1.05	57.0	1.08	89.1	1.06	77.0	1.06
PS–PVP–PB 39-35-39	38.5	1.05	34.5	1.07	38.5	1.07	42.1	1.13
PS–PVP–PB 39-180-39	38.5	1.05	180	1.07	38.5	1.07	31.8	1.10
PS–PVP–PB 16-80-17	16.4	1.04	80.1	1.05	17.4	1.07	16.4	1.09

[a] Made in Bz. [b] Made in THF. [c] Made in Bz/THF 1/1.

combined refractive index (RI) and low-angle laser light scattering monitor (Tosoh Model LS-8000) and an ultraviolet (UV) absorption monitor (Tosoh UV-8). The UV wavelength was λ = 254 nm. The elution solvent was THF, and antiadsorption columns (Tosoh G-4000 H_{XL} and G-5000 H_{XL}) were used.

PS Precursor. The weight average molecular weight M_w and the M_w/M_n ratio were determined from an elution volume calibration for the RI signals. Commercially available monodisperse PS (Tosoh TSK's) were used as the elution standards.

PS–PVP Precursor. The (apparent) M_w/M_n ratio was evaluated from the elution volume calibration made with standard PS. The content of the PVP blocks, ϕ_{PVP}, was determined from the UV and RI signal intensities, A_{RI} and A_{UV}. For dilute solutions of the PS–PVP precursors with the concentrations C, A_{RI} and A_{UV} are related to ϕ_{PVP} and ϕ_{PS} (=1 − ϕ_{PVP}) as:

$$A_{RI} = K_{RI}[\nu_{PS}\phi_{PS} + \nu_{PVP}\phi_{PVP}]C \qquad (1a)$$

$$A_{UV} = K_{UV}[\epsilon_{PS}\phi_{PS} + \epsilon_{PVP}\phi_{PVP}]C \qquad (1b)$$

Here, ν_X and ϵ_X are the RI increment and UV absorption per unit mass of the X block (X =PS or PVP), and K_{RI} and K_{UV} are the instrumental constants. The products $K_{RI}\nu_{PS}$ and $K_{UV}\epsilon_{PS}$ were determined from the data for homo PS, and $K_{RI}\nu_{PVP}$ and $K_{UV}\epsilon_{PVP}$ from the data for homo PVP. Thus, applying eq 1 to the data for these homopolymers and the PS–PVP precursor, we determined ϕ_{PVP} and ϕ_{PS}. (The proportionality between A's and C was confirmed.) The PVP block molecular weight was calculated as $M_{PVP} = (\phi_{PVP}/\phi_{PS})M_{PS}$, with M_{PS} being the PS precursor molecular weight.

PB Precursor. The PB–DPE and bare PB precursors exhibited identical RI and LS signals because the small DPE units involved in the former had practically no contribution to the signals. Those PB precursors had negligibly small UV absorption as compared to the PS or PVP blocks. For such PB precursors, M_w and M_w/M_n were determined from an elution volume calibration. Previously made and characterized monodisperse PB samples were used as the elution standards. M_w was also determined by LS. The M_w values obtained by these methods agreed well.

PS–PVP–PB Block Polymer. The (apparent) M_w/M_n ratio was evaluated from the elution volume calibration made with the standard PS. As done for the PS–PVP precursor (cf., eq 1), the content of the PB block, ϕ_{PB}, was determined from A_{RI} and A_{UV} through the relations:

$$A_{RI} = K_{RI}[\nu_{PS\text{-}PVP}\phi_{PS\text{-}PVP} + \nu_{PB}\phi_{PB}]C \qquad (\phi_{PS\text{-}PVP} = 1 - \phi_{PB}) \quad (2a)$$

$$A_{UV} = K_{UV}\epsilon_{PS\text{-}PVP}\phi_{PS\text{-}PVP}C \qquad (\epsilon_{PS\text{-}PVP} \gg \epsilon_{PB} \cong 0) \quad (2b)$$

The PB molecular weight in the PS–PVP–PB block polymer was calculated as $M_{PB}^{calc} = (\phi_{PB}/\phi_{PS\text{-}PVP})M_{PS\text{-}PVP}$, with $M_{PS\text{-}PVP}$ being the molecular weight of the PS–PVP precursor.

Table I summarizes the results of characterization for the six PS–PVP–PB three-block polymers together with those for the precursors. The sample code numbers indicate M_{PS} − M_{PVP} − M_{PB} in units of 1000. As seen in Table I, the M_{PB}^{calc} values agree well with the M_{PB} values determined independently for the PB precursors. This result indicates that the desired linear three-block polymers were successfully obtained *via* 1:1 coupling of the PS–PVP-Cl and PB–DPE⁻ precursors.

PB–PVP and PS–PVP Diblock Polymers. As done for the PS–PVP precursor, the (apparent) M_w/M_n ratio was evaluated

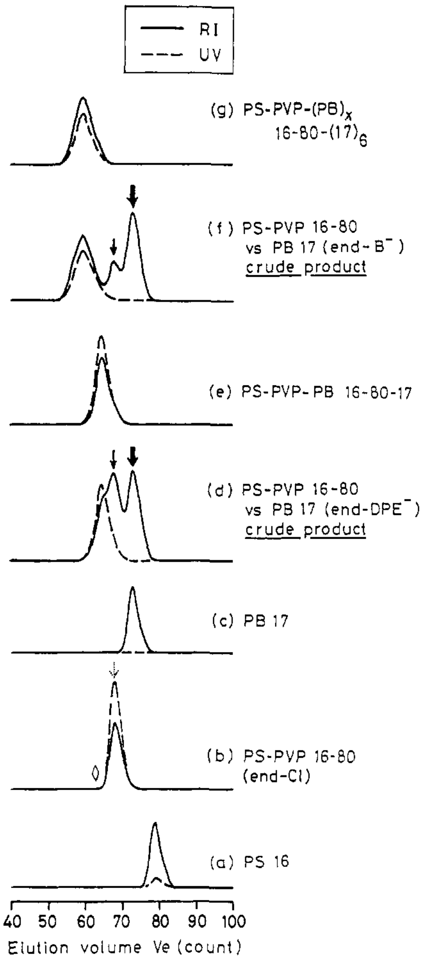

Figure 2. GPC traces obtained at various stages of the synthesis of a PS-PVP-PB 16-80-17 three-block polymer. The solid and dashed curves indicate the RI and UV signals, respectively. The signal sensitivities are the same for all traces a-g, and changes of chemical composition are visually examined through the UV/RI signal ratios in the figure. The dotted and diamond-shaped arrows for trace b indicate the locations for the PS-PVP-Cl precursor and its dimer, respectively, and the thick and thin arrows for traces d and f those for the unreacted (excess) PB precursor and its dimer, respectively.

from the elution volume calibration (made with the standard PB or PS), and the PVP block molecular weight from A_{RI}, A_{UV}, and the molecular weight of the precursor (PB or PS). Table II summarizes the results of characterization.

II-3. Measurements. The PS-PVP-PB 39-57-15 and 39-57-39 samples (cf., Table I) were adsorbed on mica from toluene solutions and subjected to the preliminary surface measurements explained below. For comparison, the measurements were made also for adsorbed layers of the PB-PVP 39-24 and PS-PVP 32-33 samples (Table II). The mica used was Grade No. 4 ASTM V-2, clear and slightly stained Muscovite, ruby red mica obtained from Asheville-Schoonmaker Mica Co. Guaranteed grade toluene (Wako Chemicals) was used after filtration with 0.2-μm Millipore filters.

Preparation of the Adsorbed Layers. First, freshly cleaved mica sheets (≅1.5 cm × 1.5 cm) were immersed in ≅200 mL of dilute toluene solutions ($C \cong 5$ μg/mL) of the PS-PVP-PB, PB-PVP, and/or PS-PVP samples for an adequate time t_{ads} (= 1.5, and 10 h) at 25 °C. Then, the mica sheets were rinsed three times with pure toluene to remove nonadsorbed (excess) chains. In each rinsing procedure, the sheets were kept in ≅300 mL of toluene for 2 h. Finally, the adsorbed layers on mica were dried under a clean nitrogen stream for at least 12 h. All these operations were made in a clean laminar flow bench, and no heat treatment (or annealing) was made for the adsorbed layers. Previous work[7,8] revealed that ultra-thin adsorbed layers (of typical thickness ≅ a few nanometers) are formed on mica with the above method.

Contact Angle Measurements. Contact angles θ were measured with a goniometer (CA-DT, Kyowa) at 25 °C for droplets of distilled water (<50 μL) placed on the as-dried PS-PVP-PB layers. For comparison, θ was measured for the water droplets on bare mica sheets as well as on homo-PS, homo-PB, and homo-PVP films of thicknesses ≅ 5 μm cast on glass plates.

Table II. Characteristics of PB-PVP and PS-PVP Diblock Polymers

code	precursor[a]		diblock polymer[b]	
	$10^{-3}M_{PB\ or\ PS}$	M_w/M_n	$10^{-3}M_{PVP}$	M_w/M_n
PB-PVP 39-24	38.5	1.07	23.7	1.05
PS-PVP 32-33	32.3	1.06	32.7	1.05

[a] Made in Bz with BuLi. [b] Made after switching the solvent from Bz to THF (cf., Scheme I).

Table III. Contact Angles θ for Water Droplets

substrate	θ (deg)
PS-PVP-PB	
39-57-15	84
39-57-39	82
homopolymers	
homo-PB	98
homo-PB	90
homo-PVP	68
mica	<10

We found that θ is the same for the PB-PVP-PB layers with t_{ads} = 5 and 10 h. This result indicates that the adsorption was saturated within 5 h, in agreement with previous results.[12] Thus, the layers with t_{ads} = 5 h were used in the following measurements.

X-ray Photoelectron Spectroscopy (XPS). For the PS-PVP-PB, PB-PVP, and PS-PVP adsorbed layers, XPS signals were examined at National Cardiovascular Center Research Institute (Suita, Japan) with a Shimazu ESCA 750 spectrometer. Integrated intensities were measured for C_{1s} and N_{1s} signals at take-off angles ϕ ranging from 90° (normal) to 15° (grazing), and they were normalized to their 90° values. The Si_{2p} signal (from mica) was also examined as a reference.

With decreasing ϕ, a path length for the photoelectron ($\propto 1/\sin\phi$) increases, and the XPS signal intensity from the bottom part of the layer decreases more rapidly than that from the top. Since the PVP block contains nitrogen but the PS and PB blocks do not, the ϕ dependence of the C_{1s}/N_{1s} signal ratio reflects a distribution of the PVP block in a depth direction: This ratio increases with decreasing ϕ if the PVP blocks are localized at the bottom.

Atomic Force Microscopy (AFM). For the PS-PVP-PB, PB-PVP, and PS-PVP adsorbed layers, AFM observations were made at Toyobo Research Center (Katada, Japan) with a Seiko Model SFA300. Silicone nitride probe tips with a radius of curvature = 250 Å (Olympus) were used. The scanning density and rate were 256 scans/μm and 3 μm/s, respectively. We changed the force level and scanning direction and repeatedly examined the AFM images for the same (or sometimes wider) section of the surface. Those images were the same, and no effects of scanning was observed.

III. Results and Discussion

III-1. Coupling Reaction. Figure 2 shows an example of the GPC traces obtained at various stages of the synthesis of the PS-PVP-PB samples for a case with M_{PS}, M_{PVP}, M_{PB} = 16.4 k, 80.1 k, 17.4 k. The solid and dashed curves indicate the RI and UV signals, with their sensitivities being the same for all traces a-g. (The LS signals are not shown to avoid complexity of the figure.) The UV absorption per unit mass is more than 10 times larger for PVP than for PS and practically 0 for PB (even with the DPE ends), while the RI increment per unit mass is nearly the same for all blocks. Thus, the UV signal is mainly due to the PVP blocks (if they exist in the sample), and the changes of the UV/RI signal ratio seen in Figure 2 indicate the changes of the chemical composition during the synthesis.

As seen for parts a and b of Figure 2, the GPC peak shifts to lower Ve side and the UV/RI signal ratio increases as the PVP block is copolymerized with the PS block and terminated with XDC. In addition to the single-chain termination that gives the end-chlorinated PS–PVP-Cl chains, *in principle* two PS–PVP⁻ anions could be coupled by XDC to yield their dimer, (PS–PVP)$_2$.[13] However, the peak b is seen at Ve for the desired PS–PVP-Cl chain (dotted arrow) that was calculated from M_{PS} and the amounts of the S and VP monomers used,[14] and no dimer is seen at the expected location (diamond-shaped arrow). Under the conditions of the termination step, the large amount of XDC (20–30 times excess to the PVP⁻ ends) and low temperature (−78 °C) coupling of the PVP anions was efficiently suppressed possibly because of their rather low reactivity and large steric hindrance.

As seen for parts b and d of Figure 2, the UV peak shifts to lower Ve side and decreases its intensity when the PS–PVP-Cl precursors are successfully coupled with the UV-inert PB–DPE precursors. The crude product (part d) contains some undesired components, excess PB–DPE (thick arrow) and (PB–DPE)$_2$ dimers (thin arrow) both exhibiting no UV absorption. In addition, through the LS signal (not shown here), we found a trace amount of undesired high molecular weight products (possibly graft-block polymers formed by a side reaction explained for parts f and g). Those undesired components were removed by fractionation to obtain the final product (part e). The M_{PB}^{calc} value of this product agrees well with the M_{PB} value of the PB precursor (cf., Table I), indicating that the desired PS–PVP–PB polymer is obtained.

For the six PS–PVP–PB samples (Table I), changes of the GPC traces were essentially the same as those shown in parts a–e of Figure 2, except for one case that involved a high molecular weight PB–DPE⁻ precursor (with M_{PB}=89.1 k). For this case, the coupling efficiently was ≅70% (but the desired PS–PVP–PB polymer was successfully recovered by fractionation). This incomplete coupling is most likely due to segregation of PS–PVP-Cl and PB–DPE⁻ precursors in the reaction mixture that is enhanced for larger M_{PB}.

In Figure 2, we have also demonstrated why the end-modified PB–PDE⁻ precursors had to be used in the coupling reaction. When *bare* PB⁻ precursors (without DEP⁻ end) are used, the UV peak of trace f for the coupling product is seen at lower Ve as compared to the UV peak of trace d. This result suggests that each PS–PVP-Cl chain reacted with more than one bare PB⁻ chain. In fact, analyses on the final product (trace g) revealed that one PS–PVP-Cl chain reacted with six PB⁻ chains. Among those six PB⁻ chains, one should have reacted with the highly reactive benzyl chloride end of PS–PVP-Cl, and the others with the 2-pyridine groups most likely via a mechanism reported by Tardi and Sigwalt[15] and Luxton et al.:[16]

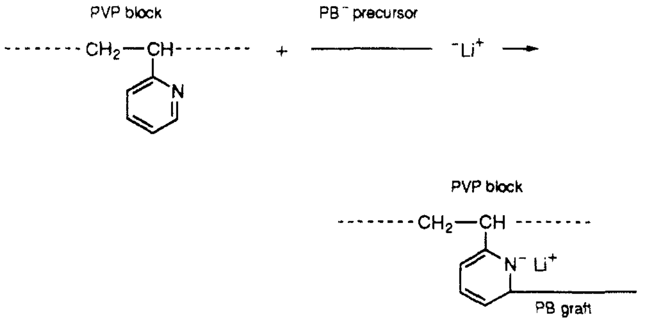

As seen for part d of Figure 2, this side reaction is efficiently suppressed and the linear PS–PVP–PB polymers are successfully obtained when the bare PB⁻ ends are converted to *less reactive* and *more bulky* DPE⁻ ends.[17]

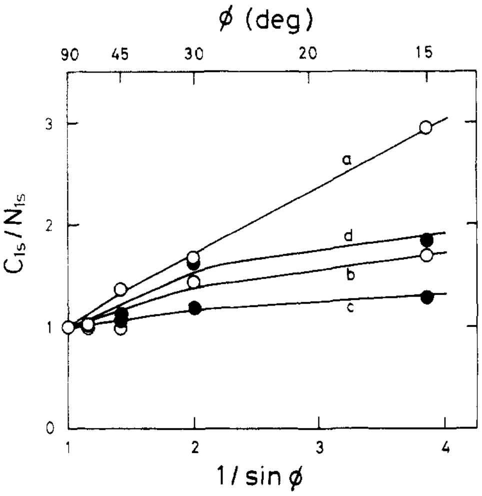

Figure 3. Dependence of the C_{1s}/N_{1s} XPS signal ratio on take-off angle ϕ for (a) PS–PVP–PB 39-57-15, (b) PS–PVP–PB 39-57-39, (c) PB–PVP 39-24, and (d) PS–PVP 32-33 adsorbed layers.

III-2. Surface Structures of PS–PVP–PB Adsorbed Layers; Preliminary Results. Table III compares the contact angles θ for the two PS–PVP–PB adsorbed layers, the homopolymer films, and mica. Clearly, θ for the adsorbed layers are much larger than θ for the PVP films and mica, and are reasonably close to θ for the homo-PS and -PB films. This result suggests that the surfaces of the PS–PVP–PB adsorbed layers are mostly covered with the PB and/or PS blocks, in harmony with the previous finding[7] that PS–PVP layer surfaces are covered with the PS blocks.

Figure 3 shows the dependence of the C_{1s}/N_{1s} XPS signal ratio on the take-off angle ϕ for the PS–PVP–PB, PB–PVP, and PS–PVP adsorbed layers. Clearly, the ratio increases with decreasing ϕ for all layers, indicating that the PVP blocks are always located at the bottom. Thus, the localization of the PS and PB blocks near the surface of the PS–PVP–PB layers is also confirmed from XPS. These blocks should be further segregated either vertically or laterally, as explained in Introduction. However, the XPS signals were indistinguishable for PS and PB blocks, and the surface structures of the PS–PVP–PB layers could not be specified from the data of Figure 3. For this problem, AFM observations provide some information.

Figure 4 shows the perspective view for the AFM images for the two PS–PVP–PB layers, and Figure 5 those for the PB–PVP and PS–PVP layers. We note that the PS–PVP–PB surfaces have many nodules of typical height ≅ 1 nm and width ≅ 20–50 nm. Similar nodules are seen for the PS–PVP surface, but not for the PB–PVP surface: The PB–PVP surface is slightly wavy but is certainly much flatter than the PS–PVP–PB and PS–PVP surfaces. This result suggests that the nodules are characteristic of the PS blocks commonly involved in the PS–PVP–PB and PS–PVP layers but not in the PB–PVP layer.

We note that the results seen in Figure 5 are consistent with the previous observation for as-dried, adsorbed layers (without heat treatment).[8] On approach of two identical PS–PVP layers in a surface force apparatus, they first touched with each other at some surface separation before a flat, molecular contact was achieved, and a compressive load could further squeeze the layers to realize this contact.[8] This result clearly indicates that the as-dried PS–PVP layers have rough surfaces (with nodules). On the other hand, for PI–PVP layers similar to the PB–PVP layer examined in Figure 5, adhesive, flat contact spontaneously

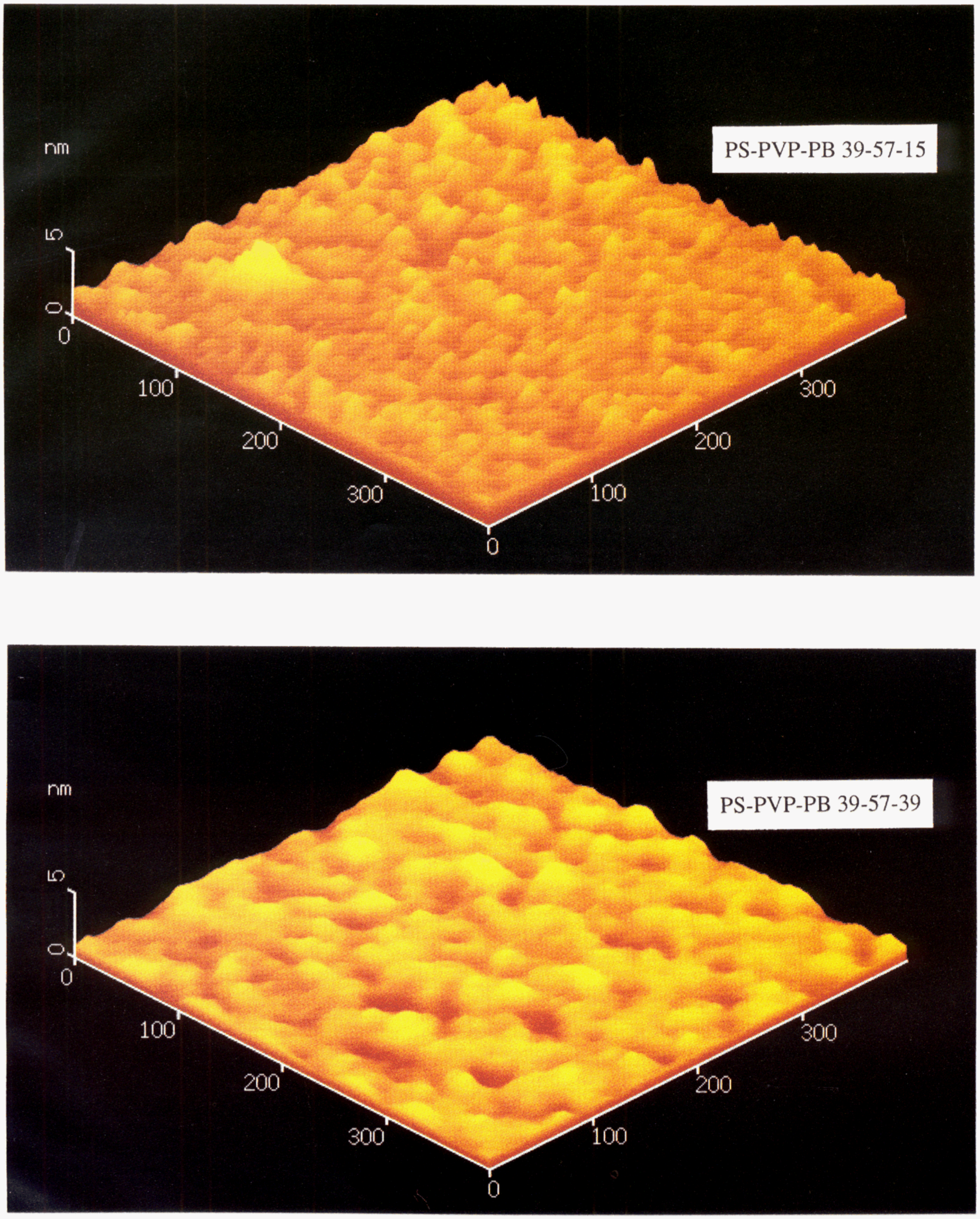

Figure 4. Perspective view of AFM images for the PS–PVP–PB 39-57-15 and 39-57-39 adsorbed layers. The origins of the vertical and horizontal axes are arbitrarily chosen. (AFM detects only the surface height profile, not the layer thickness.) Note the difference of the vertical and horizontal scales.

took place without any compressive load, and the layers could not be squeezed beyond this contact.[8] Thus, the as-dried PI–PVP layer has a molecularly flat surface, as should be the case also for the PB–PVP layer.

Structures of the as-dried layers examined in Figures 4 and 5 must have been fixed at some point during the layer preparation. When the layers are placed in toluene, the PS and/or PB blocks (anchored on mica by PVP) generally form a stretched polymer-brush with relatively low concentrations (≅ a few wt %).[8,18] As toluene evaporates, the concentration increases and, at some point, the PS blocks should be vitrified but the PB blocks do not. (For the PS–PVP–PB layers, segregation of the PS and PB blocks should also take place at some point.) On

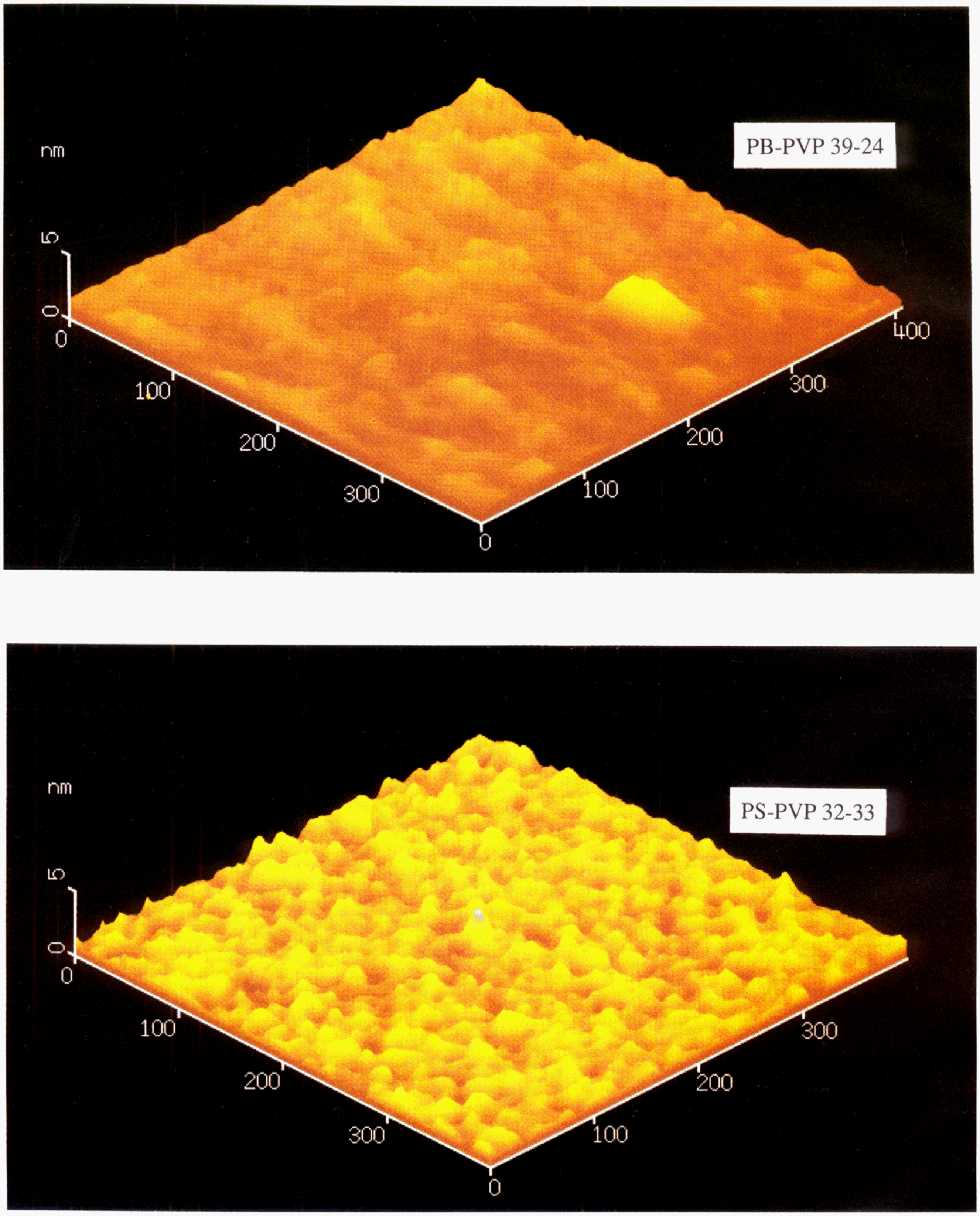

Figure 5. Perspective view of AFM images for the PB–PVP 39-24 and PS–PVP 32-33 adsorbed layers. Note the difference of the vertical and horizontal scales.

further removal of toluene, the rubbery PB blocks can change their conformation to smooth the layer surface and reduce the surface energy, while the glassy PS blocks cannot. Thus, a heterogeneity of the PS concentration distribution just before the vitrification may survive as the nodules in the as-dried layers of PS–PVP–PB and PS–PVP.

The location of the PB blocks in the PS–PVP–PB layers cannot be specified from the AFM results. However, we may speculate that the PB blocks are at the top surfaces because they are less polar and more favored by the surface energy in the nitrogen atmosphere than the PS blocks. In fact, this type of localization of nonpolar blocks is known for surfaces of bulk block polymer films.[19] Thus, the PB blocks would fill the valleys between the nodules (of possibly the PS blocks). If a sufficient amount of the PB blocks is present, they may also cover the surfaces of the nodules. However, at this moment, the adsorbed amount is not accurately known and the coverage of the nodules cannot be examined. (For completely flat layers, this amount can be determined from XPS analyses for the C_{1s} and Si_{2p} signals.[7] However, this is not the case for our PS–PVP–PB layers having wavy surfaces.)

As discussed above, the PS–PVP–PB dry layers most likely have PVP blocks at the bottom, PS blocks near the surfaces as the nodules, and the PB blocks at the top surface (between and possibly above the nodules). However, we have to acquire more data for the surface roughness and adsorbed amount to examine this structure. In this regard, it is strongly desired to experimentally distinguish the PB and PS domains. For this purpose, a surface modification of the AFM probes may be necessary. Apart from these experimental issue, thermodynamic effects on the layer structure need to be examined in more details. The structure found in this preliminary study must have been influenced by the vitrification of the PS blocks during the layer preparation, and it is important to examine the effects of annealing and the polarity of atmosphere. Finally, it is of particular interest to examine the dependence of the structures in various circumstances on molecular weights of the constituent blocks. In this regard, a difference of the nodule sizes seen for the two PS–PVP–PB layers (Figure 4) is interesting. We are now attempting to address these problems.

Acknowledgment. We thank Drs. X. J. Shao and T. Suzuki of Toyobo Research Center for their generously making the AFM observations. We thank Drs. T. Matsuda and T. Sugawara of National Cardiovascular Center Research Institute for their help on the XPS measurements. We acknowledge with appreciation the financial support for this work from Japan Society for the Promotion of Science (ENGR-194) and the National Science Foundation (NSF/INT-9016735) under a JAPAN-US Cooperative Research Program, and NSF/CTS-9107025, CTS and DMR (Polymers Program).

References and Notes

(1) See, for example, Molau, G. E. In *Block Copolymers*; Aggarwal, S. L., Ed.; Plenum Press: New York, 1970.
(2) Meier, D. J. *J. Polym. Sci.* **1969**, *C26*, 81.
(3) Helfand, E.; Wasserman, Z. R. *Macromolecules* **1976**, *9*, 829. *Ibid.* **1978**, *11*, 960.
(4) Hashimoto, T. In *Polymer Alloy*; Kotaka, T., Ide, F., Nishi, T., Ogino, K., Eds.; Kagaku Dojin: Tokyo, 1981.
(5) Bates, F. S.; Fredrickson, G. H. *Ann. Rev. Phys. Chem.* **1990**, *41*, 525. Bates, F. S. *Science* **1991**, *251*, 898.
(6) Matsushita, Y.; Mori, K.; Mogi, Y.; Saguchi, R.; Noda, I.; Nagasawa, M.; Chang, Y.; Glinka, C. J.; Han, C. C. *Macromolecules* **1990**, *23*, 4317.
(7) Parsonage, E.; Tirrell, M.; Watanabe, H.; Nuzzo, R. G. *Macromolecules* **1991**, *24*, 1987.
(8) Watanabe, H.; Tirrell, M. *Polym. Prepr.* **1989**, *20*, 387. *Macromolecules*, in press.
(9) Arai, K.; Kotaka, T.; Kitano, Y.; Yoshimura, K. *Macromolecules* **1980**, *13*, 455, 1670.
(10) Fujimoto, T.; Nagasawa, M. *Advanced Techniques for Polymer Synthesis*; Kagaku Dojin: Kyoto, 1972. Fujimoto, T., personal communication.
(11) Morton, M.; Fetters, L. J. *Rubber Chem. Technol.* **1975**, *48*, 359. Morton, M. *Anionic Polymerization: Principles and Practice*, Academic Press: New York, 1983.
(12) Watanabe, H.; Patel, S.; Tirrell, M. In *New Trends in Physics and Physical Chemistry of Polymers*, Lee, L.-H., Ed.; Plenum: New York, 1989.
(13) Another side reaction expected is the quaternization of pyridine groups due to free XDC molecules or benzyl chloride ends of the PS–PVP-Cl precursors. However, GPC traces of those precursors kept in THF at $T \leq 25$ °C remained the same even after a month, indicating negligibly slow quaternization at those *T*.
(14) At high temperatures, a side reaction of PVP anions with 2-pyridine groups may lead to branch formation. However, in this work the PVP blocks were polymerized and terminated at low temperature (−78 °C) and the *linear* PS-PVP chains were successfully obtained, as evidenced from the location of the GPC peak in Figure 2b.
(15) Tardi, M.; Sigwalt, D. *Eur. Polym. J.* **1972**, *8*, 137, 151. *Ibid.* **1973**, *9*, 1369.
(16) Luxton, A. R.; Quig, A.; Delvaux, M.; Fetters, L. J. *Polymer* **1978**, *19*, 1320.
(17) (a) It was found that bare polyisoprene (PI) anions (chemically very similar to the PB anions used in this study) reacted even with homo-PVP chains having no benzyl chloride groups to yield graft-block polymers.[17b] This result supports the discussion for the side reaction. On the other hand, practically no reaction took place for end-modified PI-DPE$^-$ and homo-PVP chains,[17b] confirming that the desired *linear* PS–PVP–PB block polymers were obtained in this study *via* coupling of the PS–PVP-Cl and PB–DPE$^-$ precursors at their ends. (b) Watanabe, H.; Amemiya, T.; Shimura, T.; Kotaka, T., manuscript in preparation for publication.
(18) Patel, S.; Tirrell, M.; Hadziioannou, G. *Colloid Surf.* **1988**, *31*, 157.
(19) Hasegawa, H.; Hashimoto, T. *Macromolecules* **1985**, *18*, 589.